Available online at www.sciencedirect.com

ScienceDirect

Developmental Biology 307 (2007) 79–91

DEVELOPMENTAL BIOLOGY

www.elsevier.com/locate/ydbio

Postsynaptic neuroligin enhances presynaptic inputs at neuronal nicotinic synapses

William G. Conroy *, Qiang Nai, Brendon Ross, Gregory Naughton, Darwin K. Berg

Neurobiology Section, Division of Biology, 0357, University of California, San Diego, 9500 Gilman Drive, La Jolla, CA 92093-0357, USA

Received for publication 13 November 2006; revised 12 April 2007; accepted 16 April 2007
Available online 21 April 2007

Abstract

Neuroligins are cell adhesion molecules that interact with neurexins on adjacent cells to promote glutamatergic and GABAergic synapse formation in culture. We show here that neuroligin enhances nicotinic synapses on neurons in culture, increasing synaptic input. When neuroligin is overexpressed in neurons, the extracellular domain induces presynaptic specializations in adjacent cholinergic neurons as visualized by SV2 puncta. The intracellular domain is required to translate the SV2 puncta into synaptic input as reflected by increases in the frequency of spontaneous mini-synaptic currents. The PDZ-binding motif of neuroligin is not needed for these effects. Together, the extracellular and proximal intracellular domains of neuroligin are sufficient to induce presynaptic specializations, align them over postsynaptic receptor clusters, and increase synaptic function. Manipulation of endogenous neuroligin with β-neurexin-expressing cells confirms its presence; repressing function with dominant negative constructs and inhibitory shRNA shows that endogenous neuroligin helps confer functionality on existing nicotinic synaptic contacts. Endogenous neuroligin does not appear to be required, however, for initial formation of the contacts, suggesting that other components under these conditions can also initiate synapse formation. The results indicate that postsynaptic neuroligin is important for functional nicotinic synapses on neurons and that the effects achieved will likely depend on neuroligin levels.

Keywords: Neuroligin; Neurexin; Nicotinic; Receptor; Synapse formation; Ciliary ganglion; PDZ

Introduction

The formation and maturation of synapses are elaborate processes requiring assembly, alignment, and stabilization of pre- and postsynaptic elements. The neuroligin (NL) family of cell adhesion molecules plays a key organizing role. The cytoplasmic domain of NL localizes with glutamate receptors in the postsynaptic cell while the extracellular acetylcholinesterase-like domain of NL interacts with neurexins (NRXs) on the presynaptic axon to form an intercellular link (Ichtchenko et al., 1995; Scheiffele et al., 2000; Dean et al., 2003; Boucard et al., 2005; Craig and Kang, 2007). NLs also have a PDZ-binding motif, enabling them to interact with PSD-95 and further facilitate assembly of postsynaptic components (Irie et al., 1997; Graf et al., 2004; Nam and Chen, 2005).

NL-1 and -3 enhance glutamatergic synapse formation while NL-2 can promote GABAergic synapse formation (Graf et al., 2004; Chih et al., 2005; Chubykin et al., 2005; Levinson et al., 2005). Recent evidence shows that interactions between NL and PSD-95 can influence the ratio of glutamatergic to GABAergic synapses formed. While the PDZ-binding domain of NL recruits PSD-95 to the synapse, it also allows PSD-95 to recruit NL. Increased PSD-95 levels may shift the distribution of neuroligin away from GABAergic and towards glutamatergic contacts, thereby influencing the ratio of excitatory to inhibitory input a cell receives (Graf et al., 2004; Prange et al., 2004; Chih et al., 2005; Levinson et al., 2005; Gerrow et al., 2006). Recent evidence, however, has challenged the view that NL actually initiates synapse formation, and instead suggests that it may act primarily to enhance subsequent maturation of glutamatergic and GABAergic synapses (Varoqueaux et al., 2006).

Nicotinic synapse formation at the vertebrate neuromuscular junction follows different rules from those operative between neurons. Agrin acting through MuSK guides postsynaptic development (Sanes and Lichtman, 2001). No role has been identified for NL. Nicotinic synapses are also found throughout the vertebrate central and autonomic nervous systems where

* Corresponding author. Fax: +1 858 534 7309.
E-mail address: wconroy@ucsd.edu (W.G. Conroy).

0012-1606/$ - see front matter © 2007 Elsevier Inc. All rights reserved.
doi:10.1016/j.ydbio.2007.04.017

they mediate excitatory transmission and influence calcium-dependent events. The roles of cell adhesion molecules at neuronal nicotinic synapses have yet to be defined.

The chick ciliary ganglion (CG) offers an attractive system for examining nicotinic synapse formation on neurons (Dryer, 1994). CG neurons have abundant nicotinic acetylcholine receptors homomeric for α7 subunits (α7-nAChRs) and localize them on somatic spines; they have heteromeric α3-containing receptors (α3*-nAChRs) concentrated in postsynaptic densities (Conroy and Berg, 1995; Williams et al., 1998; Shoop et al., 1999, 2002). Neuronal nAChRs are associated with members of the PSD-95 family (Conroy et al., 2003; Parker et al., 2004), and α7-nAChRs undergo rapid agonist-induced trafficking (Liu et al., 2005). These features recall elements of glutamatergic synapses.

We show here that the CG expresses NL-1 and that NL interactions determine the levels of nicotinic synaptic activity the neurons receive. Overexpression of NL-1 aligns presynaptic elements over nAChR clusters on the neurons and increases synaptic input to them in culture. Both the NL extracellular domain and a short cytoplasmic domain are essential, the former for recognizing NRXs in adjacent neurites and the latter for increasing synaptic function. The PDZ-binding motif is unnecessary for this enhancement. High levels of NL can enhance synapse formation and nAChR clustering even in the absence of PDZ-scaffolds. The lower levels of endogenous NL normally found in the neurons are necessary for normal nicotinic synaptic activity but are not required for the basal number of synaptic contacts seen. The results indicate that NLs can play both organizing and regulatory roles at neuronal nicotinic synapses.

Materials and methods

CG cultures

Dissociated embryonic day (E) 8 CG neurons were maintained in cell culture for 7–10 days on glass coverslips coated with poly-D-lysine, fibronectin, and lysed fibroblasts (Nishi and Berg, 1981; Zhang et al., 1994). Co-cultures of E8 CG neurons and HEK293 cells were prepared by transfecting HEK293 cells and adding them to CG cultures prepared 48 h earlier. The co-cultures were taken for analysis after an additional 48 h. Co-cultures of QT-6 fibroblasts and E8 CG neurons were prepared by transfecting QT-6 cells, fixing with 0.5% paraformaldehyde (PFA) after 48 h to prevent subsequent transfection by GFP, and then adding CG neurons and transfecting the neurons with GFP or GFP–CRIPT using Effectene (Qiagen, Valencia, CA) and culturing an additional 5 days. The cultures were then fixed with 2% PFA and stained for nAChRs or PSD-95 and Flag-tagged proteins.

Fluorescence microscopy

To label surface nAChRs and Flag-tagged proteins, neurons were incubated with the anti-α1/α3/α5 monoclonal antibody (mAb) 35 (Conroy and Berg, 1998) or goat anti-DDDDK (AbCAM, Cambridge, MA) for 15–30 min at 37 °C. After rinsing in Grey's Balanced Salt Solution, the cells were fixed with 2% PFA in 0.1 M sodium phosphate, pH 7.4, for 20 min at room temperature. To label intracellular antigens, appropriate dilutions of rabbit anti-NL (generous gift from Peter Scheiffele, Columbia University), anti-SV2 primary antibody (Developmental Studies Hybridoma Bank, University of Iowa) or anti-PSD-95 (clone K28/43; Upstate Biotechnology, Lake Placid, New York) were incubated overnight at 4 °C in PBS (150 mM NaCl, 10 mM sodium phosphate, pH 7.4) containing 5% normal donkey serum and 0.05% Triton X-100. After washing in PBS, the cells were incubated with appropriate donkey Cy3-, Cy5- or FITC-conjugated secondary antibodies (Jackson Immunoresearch Laboratories, West Grove, PA). After rinsing, the cells were viewed with a 63×, 1.4 NA objective on a Zeiss Axiovert equipped with CCD camera and digital imaging with Slidebook software (Intelligent Imaging Innovations, Santa Monica, CA). Typically, fields containing both a transfected and an untransfected neuron not contacting other neurons were randomly selected and imaged. The experimenter was blinded to the transfection. For visualization, reconstructed images were generated from *z*-axis stacks of 0.3 μm deconvolved optical sections. Control and experimental images were taken with the same exposure settings and displayed with the same dynamic range of pixel intensities for direct comparison. For quantification of receptor, SV2, or PSD-95 clusters a 2D-projection image of 3 focal planes was constructed from deconvolved images. Image intensities were thresholded, and areas of contact or cell surface were masked for analysis by highlighting the linear contact or perimeter of the cell surface with a drawing tool having a width of 12 pixels. Clusters within the masked area were defined as having at least 5 contiguous pixels with staining intensities at least twice background. Clusters of SV2 were counted manually as being aligned with nAChR clusters if they were within 2 pixels of each other. On average, 18% of the masked cell surface area on both GFP- and NL-transfected neurons was occupied by nAChR clusters (with the cluster size increased to included a 2-pixel annulus to account for the 2 pixel allowance used for determining alignment). Only 1–3% of the same surface area was occupied by SV2 clusters from adjoining neurons. Greater than 60% of the SV2 clusters, however, were aligned with nAChR clusters, indicating an association 3-fold greater than expected from random placement. Transfected HEK293 cells co-cultured with CG neurons were considered positive for multiple SV2 clusters if 3 puncta having more than 5 pixels each were found at the cell surface. Statistical significance was assessed by Student's *t*-test or ANOVA and Dunnett's post test.

RT–PCR

For detection of NL-1, cDNA was reverse-transcribed from E14-15 CG, whole brain, or trunk blood RNA (RNAeasy; Qiagen, Valencia, CA) using a Thermoscript RT–PCR System (Invitrogen Corp., Carlsbad, CA) with oligo $d(T)_{20}$ primers. The cDNAs were then used in PCR with the primers 5′-caaatgaagcacactgacttgg and 5′-ctggttgttgagtgtgaatgg corresponding to sequences in the cytoplasmic domain of the chick *NL-1* gene. The blood cDNA was competent for PCR in that several homer isoforms could be amplified. For RT–PCR cloning of full-length chick NL-1, primers 5′-caaaaattggatgataccaacc-cagtggtg and 5′-ctataccctggttgttgagtgtgaatgg were used; for full-length β-NRX-1 the primers 5′-ataagaatgcggccgcggcctccagcctgggcgctcaccaca and 5′-gctctaga-gatgttgagatcagacatagtactccttatcctt were used. PCR products of the appropriate sizes were subcloned into a pGEM-T easy vector (Promega Corp., Madison, WI) and sequenced. The full-length chick NL-1, cloned by RT–PCR from CG, was identical in sequence to that of rat and mouse NL-1, and contained the two inserts in the extracellular domain found in the mouse variant (Scheiffele et al., 2000). The β-NRX sequence used in these studies lacked the insert in splice site 4 in the LNS domain.

NL and chimeric constructs

All truncated NL and chimeric constructs were prepared by PCR and were sequenced. NL constructs were obtained from a rat NL-1 construct (N-FLAG-NL-1; Comoletti et al., 2003) having a FLAG epitope at the mature amino terminus, a 10-residue linker peptide, and the NL-1 sequence starting at Gln-46. This construct contains the two alternately spliced inserts found in the extracellular domain (Ichtchenko et al., 1996). NL-pdz, NLc54, and NLc14 include residues 46–838, 46–759, and 46–719, respectively. ExNLgpi is the same as construct NLGGPI described by Scheiffele et al. (2000), with gpi designating a glycosylphosphatidylinositol linker site. ExFmsCyNL replaces the entire extracellular and transmembrane sequences of NL with the extracellular and transmembrane domains of the mouse proto-oncogene *fms-c* (M-CSF-1 receptor). ExFmsCyNL-pdz was made by introducing a stop codon five residues before the authentic stop codon in ExFmsCyNL. The full-length chick NL-1 cDNA containing the two alternately spliced inserts in the extracellular domain

was subcloned into the N-FLAG vector starting at Gln-46. GFPCyNLc54 was made by inserting the first 54 amino acids of the rat NL-1 cytoplasmic domain (amino acids 706–759) in frame at the carboxyl terminus of green fluorescent protein (GFP) in the vector pEGFP-C1 (Clontech, Mountain View, CA).

RNA inhibition

A short hairpin RNA (shRNA) cassette (GenScript, Scotch Plains, NJ) was constructed targeting the NL sequence GGATGTAGTTTCCACCTATGT with the intention of suppressing NL expression. A control shRNA was constructed targeting the scrambled sequence CAACTTGAAGTAACCTAACCA. Both the active and control shRNA cassettes were subcloned into the expression vector pRNAT-U6.1/Neo (Genscript) that uses a U6 promoter for shRNA expression and carries the GFP marker under control of a CMV promoter to track the transfection.

Transfections

Transient transfections were performed on HEK293 and QT-6 cells by calcium phosphate precipitation (Conroy and Berg, 1998). CG neurons were transfected at the time of plating as previously described (Conroy et al., 2003) using the transfection reagent Effectene (Qiagen, 0.25–0.5 μg DNA/well, 1:25 ratio of DNA/Effectene). After 24 h the medium was replaced with fresh medium. Cultures were analyzed after 7–10 days. Typical transfection efficiencies were 1–2%.

Pull-down assays and immunoblots

NL from Triton X-100 lysates of E17-18 CG was affinity purified on β-NRX fusion proteins bound to Protein-G-Agarose (Boucard et al., 2005). The β-NRX fusion protein, derived from a β-NRX cDNA cloned by RT-PCR from E14 to E15 CG (see above), contained the extracellular amino acid sequences from 1 to 300 of the mature chick β-NRX-1 polypeptide lacking splice site 4 and including splice site 5 cloned into the expression vector Signal pIgplus having the signal peptide from CD33 at the amino terminus and the human IgG1 Fc tail at the carboxy terminus. The fusion protein construct was transfected into HEK293 cells, and the medium containing the secreted fusion protein was harvested after 3 days and applied to Protein-G–agarose. CG lysates in 1% Triton X-100, 50 mM Tris pH 7.4, 150 mM sodium chloride, and 1 mM calcium chloride were applied. After overnight incubation the affinity matrix was washed and bound proteins eluted with SDS–PAGE sample buffer. Medium from HEK293 cells transfected with the Signal pIgplus vector, expressing only the human IgG1 Fc, served as a negative control.

Samples for immunoblots were subjected to SDS–PAGE and electroblotted to nitrocellulose, and probed with anti-NL mAb 4F9 (Synaptic Systems, Germany), followed by goat anti-mouse secondary antibodies. Signals were visualized by enhanced chemiluminescence.

Electrophysiology

Whole-cell patch-clamp recordings were obtained from E8 CG neurons after 5–8 days in dissociated cell culture as described (Chen et al., 2001; Nai et al., 2003). Transfected cells were identified by GFP fluorescence. Cells were maintained at 37 °C and voltage-clamped at −70 mV to monitor spontaneous synaptic activity. Recording conditions, solution contents, and criteria for accepting data were those described previously (Chen et al., 2001; Nai et al., 2003). Tetrodotoxin (TTX) when present was included in the medium at 0.5 μM. Whole-cell nicotinic responses were obtained at the end of each recording session by rapid application of 20 μM nicotine as described (Conroy et al., 2003). Spontaneous miniature excitatory postsynaptic currents (mEPSCs) were analyzed by Mini Analysis Program software (Synaptosoft, Inc., Decatur, GA); whole-cell responses were analyzed as described (Nai et al., 2003). Electrical noise was typically 3–4 pA in amplitude; TTX-resistance, shape, and amplitude ≥10 pA were the criteria for identifying mEPSCs. For analysis of mEPSC frequency and amplitude distributions, data were graphed in cumulative probability plots, and statistical significance was determined by Kolmogorov–Smirnov Two-Sample Test. For comparisons among populations of transfected cells, results were first normalized to controls in each case, and the ratios used to construct means±SEM; statistical significance was assessed by Student's *t*-test or ANOVA and Dunnett's post test.

Materials

White leghorn chick embryos were obtained locally and maintained in a humidified incubator. All other reagents were purchased from Sigma (St. Louis, MO), unless otherwise indicated. Rat NL-1 and mouse NL-gpi expression constructs were kindly provided by Thomas Sudhof (University of Texas Southwestern Medical Center, Dallas, TX), Palmer Taylor (University of California, San Diego, CA), and Davide Comoletti (University of California, San Diego, CA). Rabbit antiserum to a NL fusion protein was a generous gift from Peter Scheiffele (Columbia University). Signal pIgplus vector was kindly provided by Brad Spiller (Henry Wellcome Research Institute, Cardiff, UK).

Results

Neuroligin-1 in chick CG

The chick CG expresses NL-1. RT–PCR analysis of E14 CG cDNA revealed transcript for NL (Fig. 1A), and sequencing confirmed it to be NL-1. NL-1 transcript was also found in whole chick brain cDNA tested as positive control, and was absent from peripheral blood cDNA tested as a negative control. Western blot analysis demonstrated NL-1 protein in the CG (Fig. 1B). The protein could be depleted from ganglion lysates by absorption specifically with a fusion protein containing the extracellular domain of β-NRX as expected for NL (Ichtchenko et al., 1995; Boucard et al., 2005), and could be recovered from the fusion protein complex (Fig. 1B). A second anti-NL antibody directed against a different region of the protein (P. Scheiffele, personal communication) labeled the same component (not shown), providing further corroboration of identity. The sensitivity of currently available antibodies was not sufficient to visualize endogenous NL in CG neurons unless special steps were taken. One successful approach involved culturing CG neurons with HEK cells expressing flag-tagged β-NRX and then staining for NL as done with hippocampal neurons (Graf et al., 2004; Nam and Chen, 2005). HEK cells expressing β-NRX induced brightly stained clusters of NL at sites of contact with the CG neuron (Fig. 1C). Control HEK cells expressing GFP were without effect. These data demonstrate NL expression in CG neurons and suggest a role for it in the development of nicotinic synapses.

NL induction of nicotinic synapses

To determine whether NL can induce nicotinic synapses on neurons, we first transfected a Flag-tagged NL-1 construct (NL) into HEK293 cells and co-cultured the cells with CG neurons, following a strategy used in previous investigations of NL effects on glutamatergic synapses (Scheiffele et al., 2000; Chubykin et al., 2005). NL-transfected cells, but not GFP-actin-transfected cells (negative control), induced presynaptic specializations from adjacent neurites as indicated by SV2 staining within processes stained for neurofilament protein (Figs. 2A, C). The SV2 puncta suggested localization of presynaptic components. The extracellular domain of NL was

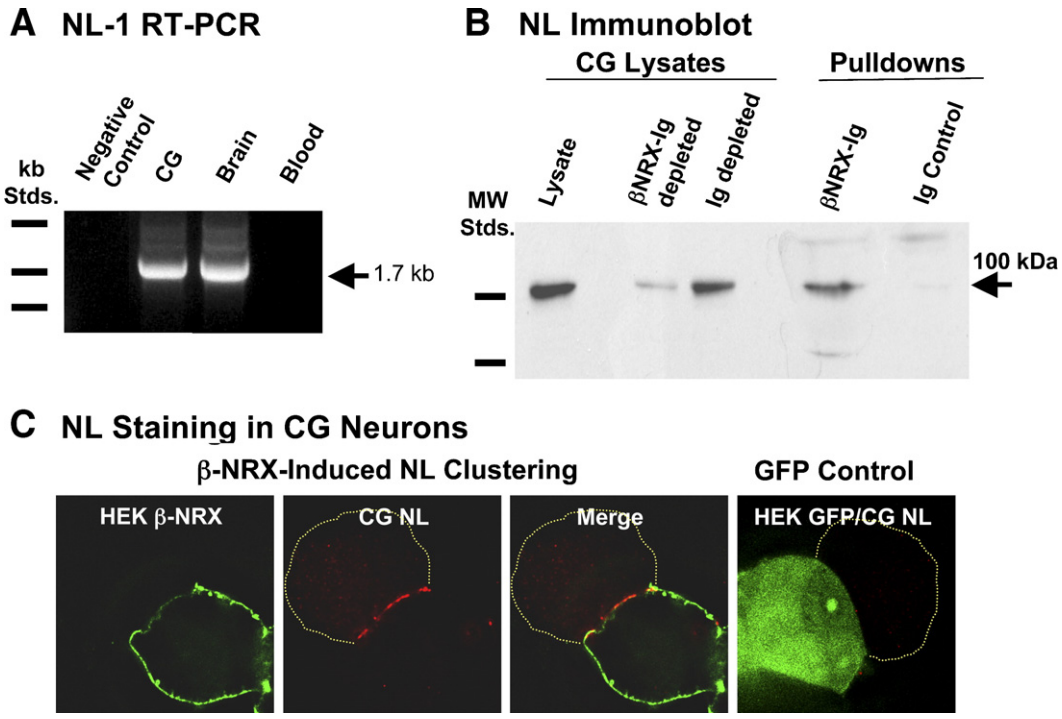

Fig. 1. NL-1 expression in CG. (A) RT–PCR detection of NL-1 transcripts in CG and brain. Sequencing confirmed the identity of the product. Omission of cDNA (negative control) and substitution of blood cDNA yielded no NL-1 transcript by RT–PCR. Size standards were 2.0, 1.6, and 1.0 kb, top-to-bottom; the 1.7 kb band is the size expected for NL-1 (arrow). (B) Immunoblot detection of NL proteins in CG extracts and their sequestration by β-NRX. Detergent-solubilized CG extracts (CG lysates) were either analyzed directly on Western blots (Lysate) or after depletion with either a tethered fusion protein containing the extracellular sequence of β-NRX (β-NRX-Ig Depleted) or a tethered negative control (Ig Depleted). The bound material was eluted and analyzed as well (Pulldowns). The β-NRX fusion protein efficiently absorbed the NL (β-NRX-Ig); the control did not (Ig Control). Dilution of the Lysate accounts for the slight decrease seen when comparing Lysate with Ig Depleted. MW, molecular weight standards of 97 and 66 kDa; the component detected by probing with anti-NL antibody had the size expected for chick NL, about 100 kDa (arrow). (C) Endogenous NL in CG neurons. HEK293 cells transfected with Flag-tagged β-NRX were co-cultured with CG neurons for 48 h and immunostained with anti-Flag antibodies (green) and co-stained for NL (red). Contact of β-NRX-expressing HEK293 cells with CG neurons induced dramatic clustering of NL (first 3 panels). Contact of CG neurons with HEK293 cells expressing GFP (GFP Control) showed no NL clustering (last panel). Yellow hatched lines outline the CG somas.

needed for the presynaptic effects; exchanging the extracellular domain of NL with that from the proto-oncogene *Fms* (ExFmsCyNL, see also Fig. 6) did not show increased SV2 clusters (Figs. 2C, D).

This prompted us to repeat the experiments, this time transfecting CG neurons and examining the impact on contacts with untransfected neurons. Again, NL-transfected neurons, but not GFP-transfected neurons, increased deposition of SV2 puncta in adjacent neurites from untransfected neurons (Figs. 3A, B). Quantification of the effect was obtained by constructing a short *z*-stack of 3 optical sections through the middle of the transfected neuron (Figs. 3C, D), and then measuring the number of SV2 puncta contacting the soma, the number of α3*-nAChR clusters on the soma, and the incidence of SV2 puncta aligned with the receptor clusters all within this short *z*-stack (Fig. 3E). The analysis showed that NL transfection doubled both the number of SV2 puncta and the incidence of SV2 puncta overlying the receptor clusters, and did so without changing the number of receptor clusters. Though the alignment of SV2 clusters with nAChR clusters was far from complete, it was at least 3-fold greater than expected from random distribution. Thus for GFP-transfected neurons the proportion of the surface area (masked perimeter of the cell) occupied by nAChR clusters (33±3 per cell) was 18% on average while the proportion for SV2 clusters (13±1 per cell) was 1.5%. In contrast, the proportion of SV2 clusters aligned with nAChR clusters was 62%. Similarly for NL-transfected neurons, the number of nAChR clusters remained unchanged while the number of SV2 clusters doubled, occupying 3% of the surface mask; the proportion of SV2 clusters aligned with nAChR clusters was 64%. The results suggest that NL-1 not only increases the number of SV2 clusters contacting the cell, but also increases the number of synaptic contacts as reflected in SV2 alignment with nAChR clusters on the neuron.

Patch-clamp recording was performed on transfected CG neurons to determine if the NL-induced increase in SV2 puncta correlated with an increase in synaptic events. Indeed, neurons expressing the NL construct had significantly more spontaneous mEPSCs recorded in the presence of TTX than did control neurons transfected with the GPF construct (Fig. 4A). The mEPSCs were completely blocked by 100 μM d-TC (Fig. 4A), as expected for nicotinic events. Cumulative probability plots for the inter-event interval showed that NL-transfected neurons had spontaneous mEPSCs at a greater frequency, i.e. short inter-event interval, than did control GPF-transfected cells (Fig. 4B, left panel; $p<0.001$). Mean frequencies of 3.1±0.9 and 0.7±0.1 events/s were found for NL- and GPF-transfected cells, respectively. No difference was seen in the amplitude distribu-

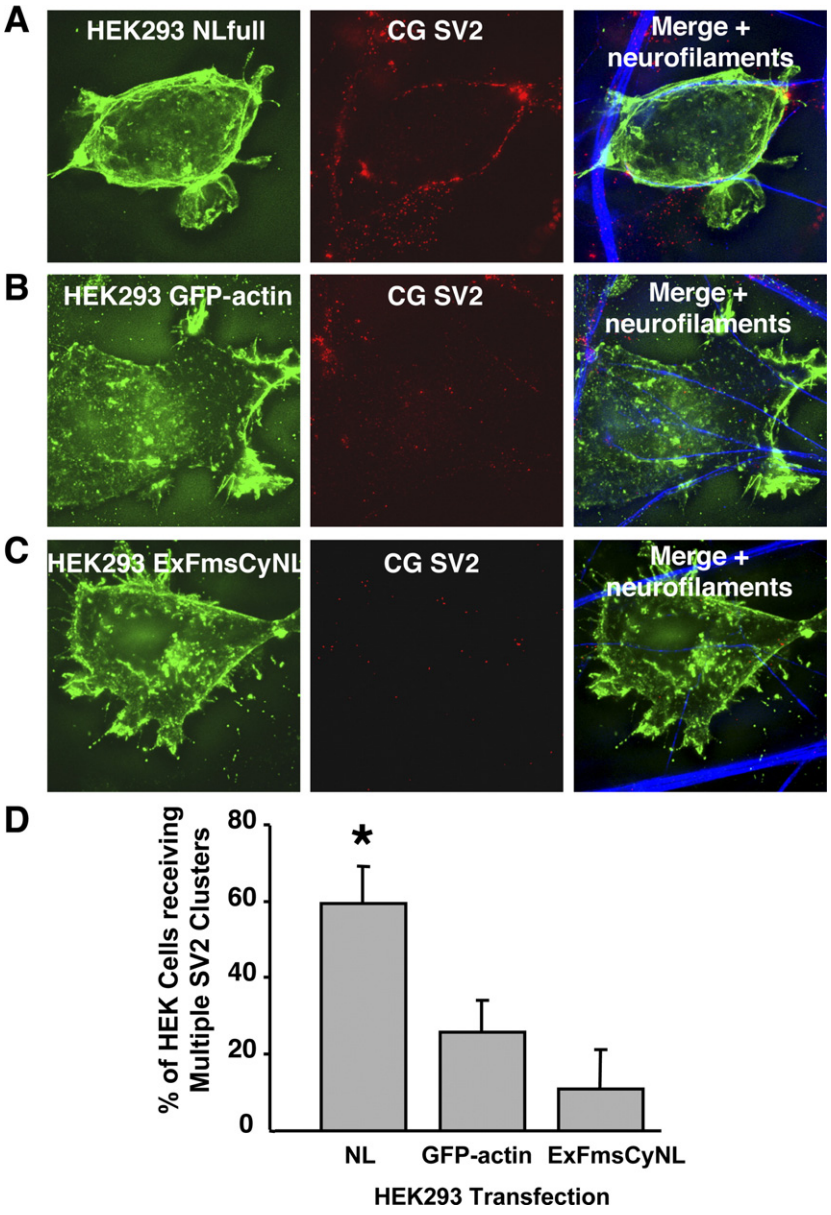

Fig. 2. Synaptogenic effects of NL on CG neurons. HEK293 cells expressing NL-1 in co-culture with dissociated E8 CG neurons induced presynaptic specializations in adjacent CG neurites. (A) HEK293 cells transfected with Flag-tagged NL-1 were co-cultured with CG neurons for 48 h and immunostained with anti-Flag antibodies (green) and co-stained for neuronal SV2 antigen (red) and neurofilaments (blue). Large bright clusters of SV2 are seen contacting NL-1-expressing HEK293 cells. (B) HEK293 cells expressing GFP-actin (green), co-cultured with CG neurons and immunostained for neuronal SV2 (red), showed only occasional smaller contacts. (C) Exchanging the extracellular domain of NL with that from the proto-oncogene *Fms* (ExFmsCyNL, green) did not show increased SV2 clusters (red) indicating that the extracellular domain of NL was needed for the presynaptic effects. Neurofilament staining (blue) in merged images shows neurite contacts. Scale bar = 10 μm. (D) Quantification of SV2 clusters shows a significant effect of NL-expressing cells (*$p < 0.05$; $n = 3$ experiments with 20–50 HEK293 cells per experiment).

tion of mEPSCs in NL-transfected cells compared to control cells (Fig. 4B, right panel). Event histograms for mEPSC amplitude indicated that it was unlikely many events were lost in the noise; both in control and in NL-transfected cells, the event incidence peaked at values well above the minimum detectable (data not shown). A greater proportion of mEPSCs in NL-transfected cells displayed rapid decay kinetics, suggesting a dependence on α7-nAChRs. The frequencies of both slowly and rapidly decaying mEPSCs, however, were increased by NL transfection, indicating that the effect was not confined to one class of nicotinic receptors. NL-transfection did not change the whole-cell response to exogenously applied nicotine (mean peak amplitude: 800 ± 70 and 820 ± 150 pA for 13 control and 12 NL-transfected cells, respectively). The results are consistent with NL transfection having caused an increase in functional nicotinic synaptic contacts on the neurons.

The synaptic contacts, for the most part, must involve presynaptic specializations on neurites from untransfected neurons abutting on the postsynaptic surface of the NL-transfected cell. Only 1–2% of the neurons are normally

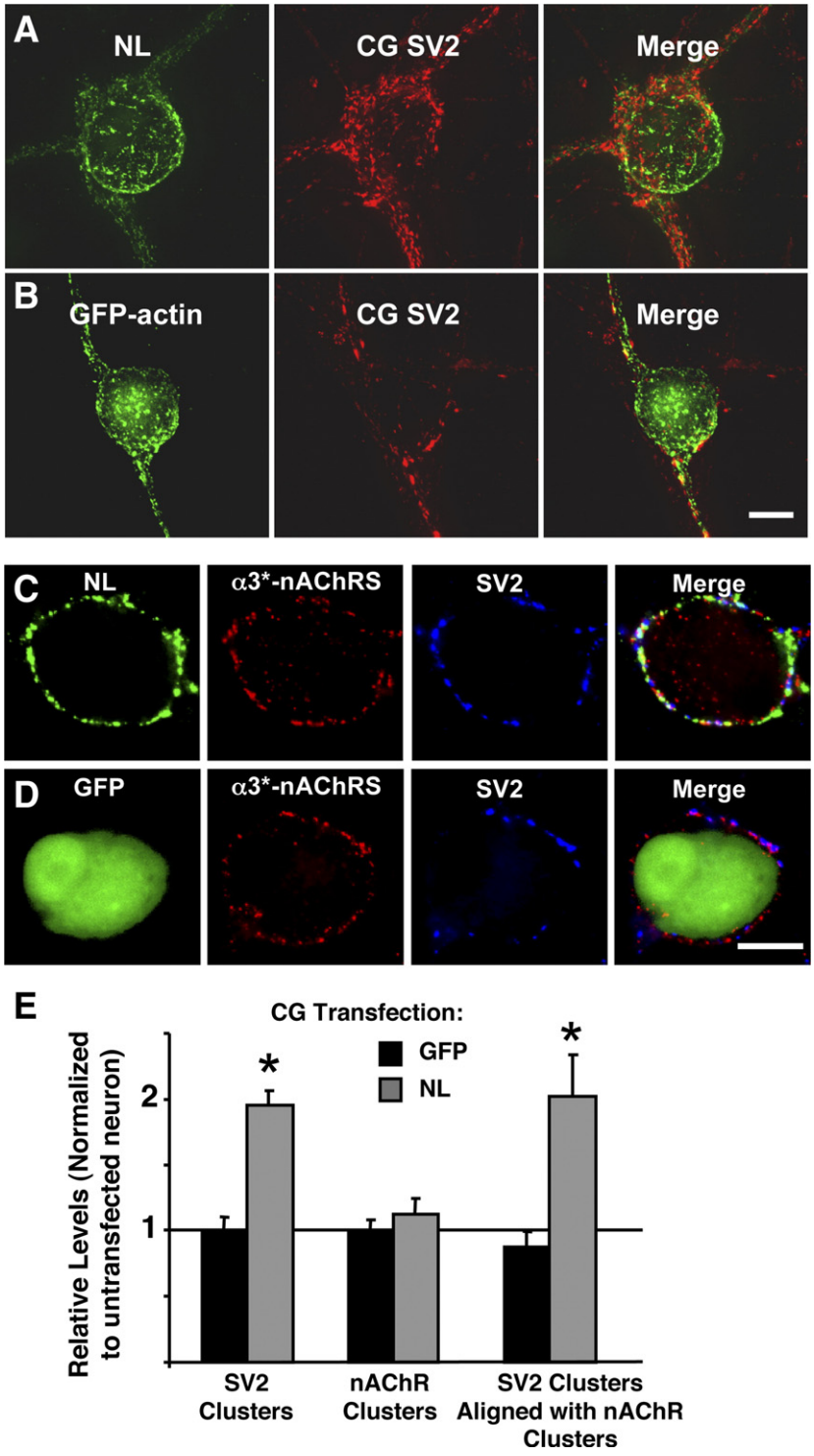

Fig. 3. NL transcellular induction of SV2 puncta and alignment over nicotinic receptor clusters. Dissociated E8 CG neurons were transfected with constructs encoding either NL (A) or GFP-actin as a negative control (B), and 7 days later were immunostained for NL (green) and SV2 (red). NL-transfected cells, viewed as a collapsed *z*-stack of optical sections, were seen to receive on average substantially more SV2 puncta than did the transfected controls. Viewing optical sections after triple staining for NL (green), α3*-nAChRs (red), and SV2 (blue) showed that NL transfection aligned a significant proportion of the SV2 puncta over receptor clusters (C), in contrast to control transfections (D). Scale bars: 10 μm. (E) Clusters of α3*-nAChRs and SV2 were quantified and compared to the levels on untransfected cells on the same coverslip (*$p<0.05$, $n=5$ experiments with 5–6 neurons per experiment).

transfected in CG cultures, and they are widely dispersed among the abundant untransfected neurons. Most, if not all, of the synaptic input received by a cell comes from other neurons, rather than from autapses. This can be inferred from examining the EPSCs evoked by spontaneous action potentials in the cultures (Conroy et al., 2003). TTX reversibly blocked the EPSCs as expected for action potential-induced events, but voltage-clamping the postsynaptic neuron did not. This was also

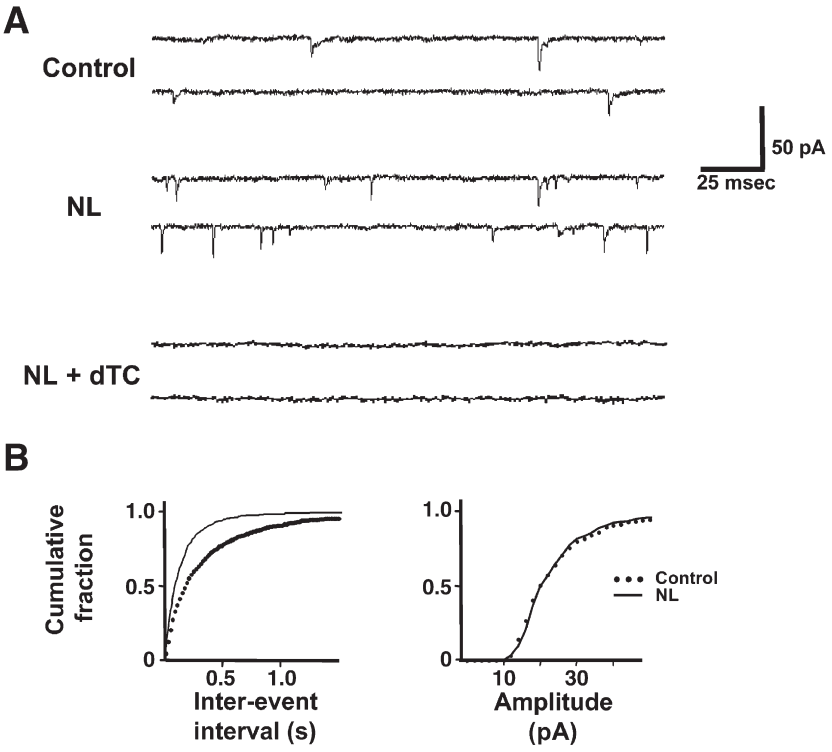

Fig. 4. Increased mEPSCs in neurons transfected with NL. (A) GFP-transfected neurons had fewer spontaneous mEPSCs in the presence of TTX (Control) than did NL-transfected neurons (NL). The mEPSCs were nicotinic as shown by blockade after incubation with 100 μM d-tubocurarine (dTC). Two traces are shown in each case. (B) Cumulative probability plots demonstrated a shortening of the inter-event interval for mEPSCs in NL-transfected cells (NL) compared to GFP-transfected cells (Control), indicating an increase in mEPSC frequency (left panel; $p<0.001$). A comparison of amplitude distributions showed that mEPSCs in NL-transfected cells were similar to controls (right panel; $n=2194$ and 10056 events for control and NL, respectively).

true for NL-transfected neurons (not shown). The SV2 and mEPSC data strongly argue for NL-transfection increasing the number of synaptic contacts made onto the transfected cell, and those contacts represent largely, if not exclusively, interneuronal contacts.

NL interactions with β-NRX

In glutamatergic pathways, NL-1 in the presumptive postsynaptic membrane interacts with β-NRX in the presynaptic terminal to promote synapse formation (Dean et al., 2003; Chih et al., 2005). To examine the possibility that β-NRX performed a similar role here, we first carried out RT–PCR analysis to reveal full-length β-NRX transcript in E14 CG cDNA. The β-NRX cDNA was then cloned and used to generate a Flag-tagged β-NRX construct for transfecting CG neurons. Immunostaining CG cultures showed that neurites from neurons transfected with β-NRX were capable of inducing α3*-nAChR/PSD-95 co-clusters in untransfected neurons at points of contact (Fig. 5A). In contrast, neurites from GFP-transfected neurons, analyzed as a negative control, showed little change in receptor clusters or PSD-95 puncta (Fig. 5B). Quantifying the relative intensities of immunostaining demonstrated a significant increase in both PSD-95 and α3*-nAChR staining juxtaposed to neurites with β-NRX vs. control neurites containing GFP and endogenous levels of β-NRX (Fig. 5C). Similar differences were seen for PSD-95 and α3*-nAChR staining on neurons overlaid by HEK293 cells transfected with β-NRX vs. GFP as a negative control (Fig. 5D). The results (Figs. 1C and 5) show that β-NRX can participate in transcellular interactions to cluster presumptive postsynaptic components on adjacent untransfected CG neurons in culture. The endogenous transcellular partner of β-NRX is very likely to be NL.

Functional domains of NL for nicotinic synapses

The experiments with β-NRX suggested that the extracellular portion of NL, which includes the β-NRX binding domain, would be essential for NL-induction of nicotinic synapses in CG cultures. A series of constructs was made to test this and other domains (Fig. 6A). A Flag epitope was attached to the amino terminus in each case to facilitate immunostaining of intact cells, as in the case of Flag-tagged full-length NL-1. Each construct was tested by transfecting CG neurons in culture, and using patch-clamp recording 5–7 days later to monitor spontaneous mEPSCs in the presence of TTX. Both the frequency and amplitude of mEPSCs were measured and expressed as a percent of control values; these normalized values were then averaged for a given construct. Controls combined neurons transfected with GFP and untransfected neurons from cultures expressing NL-1 variants because no differences were detected in mEPSC properties for these two classes of cells. Comparable surface expression, determined by immunostaining, was found for all of the NL variants; no differences were seen among the constructs

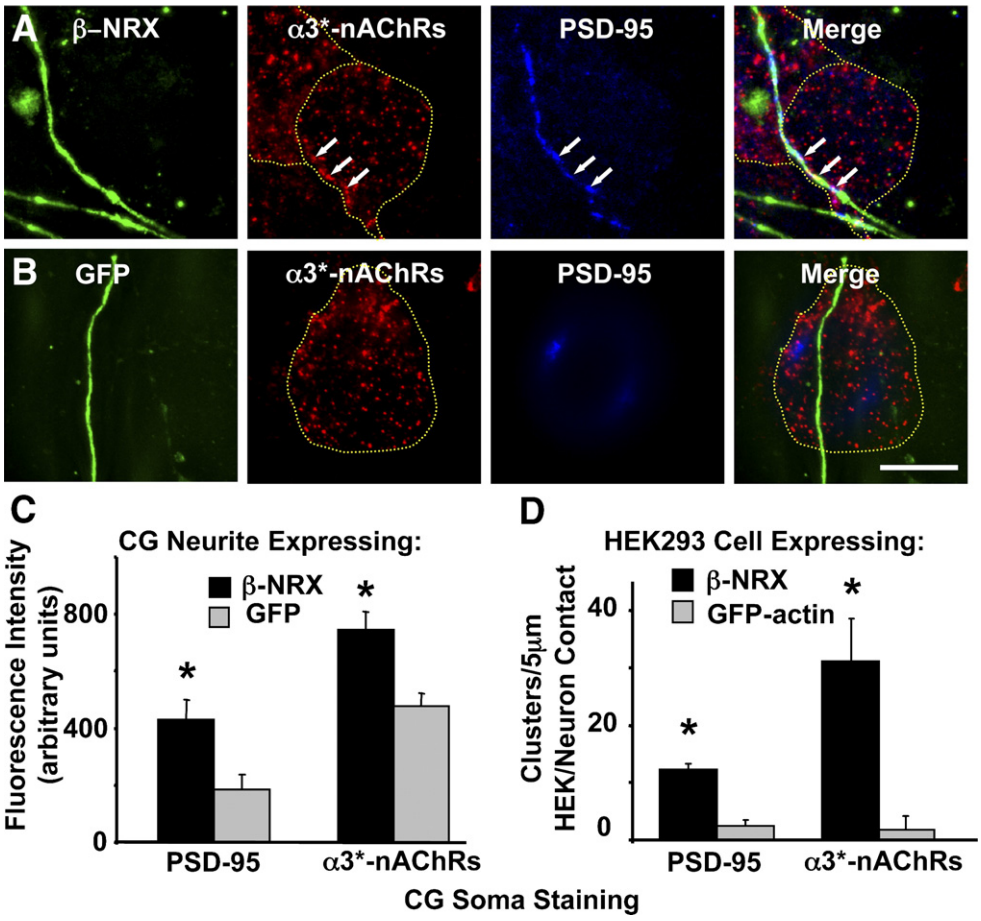

Fig. 5. Transcellular induction of α3*-nAChR and PSD-95 clusters by β-NRX. (A) Transfecting CG neurons with β-NRX and triple staining for β-NRX (green), α3*-nAChR (red), and PSD-95 (blue) 7 days later shows that neurites over-expressing β-NRX can induce large co-clusters of PSD-95 and α3*-nAChRs (arrows) in adjacent untransfected neurons (yellow hatched lines). (B) Neurites expressing GFP as a negative control show typical endogenous clustering. Scale bar: 10 μm. (C) Quantifying relative intensities of α3*-nAChR and PSD-95 staining at sites where neurites from transfected neurons contact untransfected neurons shows a significant effect of β-NRX (*$p<0.05$, $n=4$ experiments with 5–10 neurons per experiment). (D) Co-cultures of transfected HEK293 cells and untransfected E8 CG neurons also show significant effects of β-NRX on α3*-nAChRs and PSD-95 staining at sites of HEK contact with neurons (*$p<0.05$, $n=3$ experiments with 3–5 neurons per experiment).

in the mean size of the mEPSCs they produced relative to controls.

The extracellular domain was essential for increased frequency of mEPSCs. Substituting the extracellular domain of the proto-oncogene *Fms* eliminated the ability of the encoded protein (ExFmsCyNL) to enhance the frequency (Fig. 6B). In fact, it acted as a dominant negative, reducing the basal frequency. Removing the terminal intracellular PDZ binding domain (ExFmsCyNL-pdz) did not eliminate the dominant negative activity. The results implied that some portion of the NL cytoplasmic domain might also be necessary to produce mEPSC enhancement, and that overexpressing a version of it coupled to an inactive extracellular domain might interfere with the ability of endogenous NL to promote nicotinic synapse formation. Indeed, expressing a truncated cytoplasmic segment fused with GFP (GFPCyNL54) acted as a dominant negative, reducing mEPSC frequency as seen with ExFmsCyNL and ExFmsCyNL-pdz (Fig. 6B). Testing a series of constructs showed that systematically removing cytoplasmic segments from the full-length NL construct was without effect until the proximal 14 amino acid segment was deleted. Thus NL, NL-pdz, NLc54, and NLc14 each increased mEPSC frequency, but ExNLgpi did not (Fig. 6B). ExNLgpi did, however, increase the number of SV2 puncta abutting the transfected cell, though it failed to align them with α3*-nAChR clusters (data not shown). The results indicate that the extracellular domain is sufficient to interact with a component (presumably β-NRX) on the presumptive presynaptic terminal to induce accumulation of presynaptic elements. A second domain, however, involving some portion of the transmembrane domain and first 14 amino acids of the cytoplasmic domain is required to align the accumulated presynaptic elements over postsynaptic receptor clusters. This alignment is necessary to produce functional synaptic contacts as reflected in mEPSC frequency.

PDZ-independent NL effects

NL-1 has a PDZ binding motif and is known to interact with PSD-95 (Irie et al., 1997). The finding that NL-pdz, an NL-1 construct lacking the PDZ binding domain, could still induce

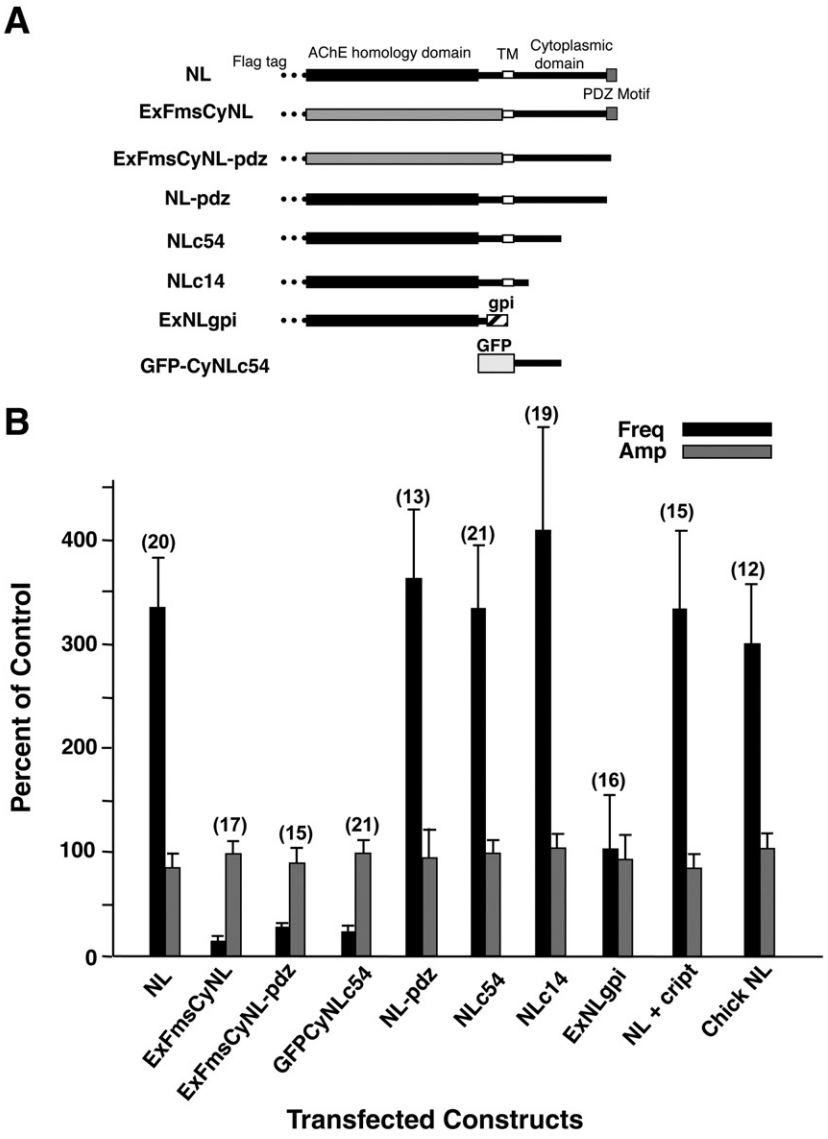

Fig. 6. Required NL domains for induction of nicotinic synapses. (A) NL constructs were prepared for transfection of E8 CG neurons in culture. NL, rat NL-1 full length with an 8-amino-acid FLAG epitope fused on the N-terminus; ExFmsCyNL, NL-1 construct in which the extracellular domain was replaced by the extracellular domain of Fms; ExFmsCyNL-pdz, ExFmsCyNL lacking the C-terminus PDZ-binding motif of NL-1; NL-pdz, NL-1 lacking the 5-amino-acid C-terminus representing a PDZ-binding motif; NLc54 and NLc14, NL-1 truncated after the first 54 and 14 amino acids, respectively, of the cytoplasmic domain; ExNLgpi, extracellular AChE-like domain of NL-1 with a gpi linkage site at the C-terminus; GFPCyNLc54, GFP fused to the first 54 amino acids of the cytoplasmic domain of NL-1. Flag tag, 8 amino acids attached at the N-terminus; AChE homology domain, extracellular domain of NL-1 homologous to the equivalent region of AChE; TM, transmembrane domain; Cytoplasmic domain, cytoplasmic portion of NL-1; PDZ motif, PDZ-binding motif; GFP, green fluorescent protein sequence. (B) Changes in mEPSC frequency caused by individual NL-1 constructs. The frequency and amplitude of mEPSCs recorded (in TTX) from neurons 5–8 days after transfection with the indicated NL-1 constructs were expressed as a percent of the values obtained from control neurons in the same cultures and then averaged across experiments to obtain mean±SEM for the normalized values (*n* indicates the number of neurons). CRIPT refers to a GFP-CRIPT construct that disperses PDZ-scaffold proteins. Chick NL, chick full-length NL-1. All of the normalized values for frequency, except for ExNLgpi, were significantly different ($p<0.05$) from control (100%) where control represents cells transfected with GFP and untransfected cells; none of the normalized values for amplitude were significantly different from control (100%). The results indicate that extracellular and proximal cytoplasmic sequences of NL are necessary to enhance mEPSC frequency, while dominant-negative effects are observed for constructs having only the NL cytoplasmic sequence or the cytoplasmic sequence attached to an inappropriate extracellular sequence. PDZ interactions are not required for the effects.

functional nicotinic contacts (Fig. 6B) suggested that interaction with the PDZ-scaffold was secondary to the initial stages of NL-induced synaptogenesis. This was tested further by co-transfecting neurons with the NL-1 construct along with either a CRIPT construct to disrupt PDZ-scaffolds (Conroy et al., 2003) or a GFP construct as a control. Under these conditions, CRIPT disperses PDZ-scaffolds as shown by immunostaining, diminishes spontaneously evoked EPSCs as monitored by patch-clamp recording, and reduces intracellular downstream signaling, but does not alter the pattern of α3*-nAChR clusters as shown by immunostaining (Conroy et al., 2003). In the present experiments, the CRIPT construct did not prevent NL from enhancing mEPSC frequency (Fig. 6B) even though immunostaining confirmed dispersal of the PDZ-scaffolds (not

shown). Most transfections were performed with rat NL constructs because of availability, but to ensure that the CRIPT results were not species-dependent, we replicated the key results with the chick NL-1 construct. Transfecting neurons with a full-length NL-1 chick construct (Chick NL) produced an increase in mEPSC frequency comparable to that seen with rat (Fig. 6B). Co-transfecting with chick NL and GFP-CRIPT still caused a 2.1-fold increase ($p<0.05$; $n=6$ cells) in mEPSC frequency over controls. Thus enhanced NL expression can override the decrement in nicotinic input previously shown to result from PDZ dispersal in CG neurons (Conroy et al., 2003).

Immunostaining transfected CG neurons supported a similar conclusion. Co-staining for α3*-nAChRs and transfected NL showed partial overlap of the two kinds of clusters (Fig. 7A). Co-

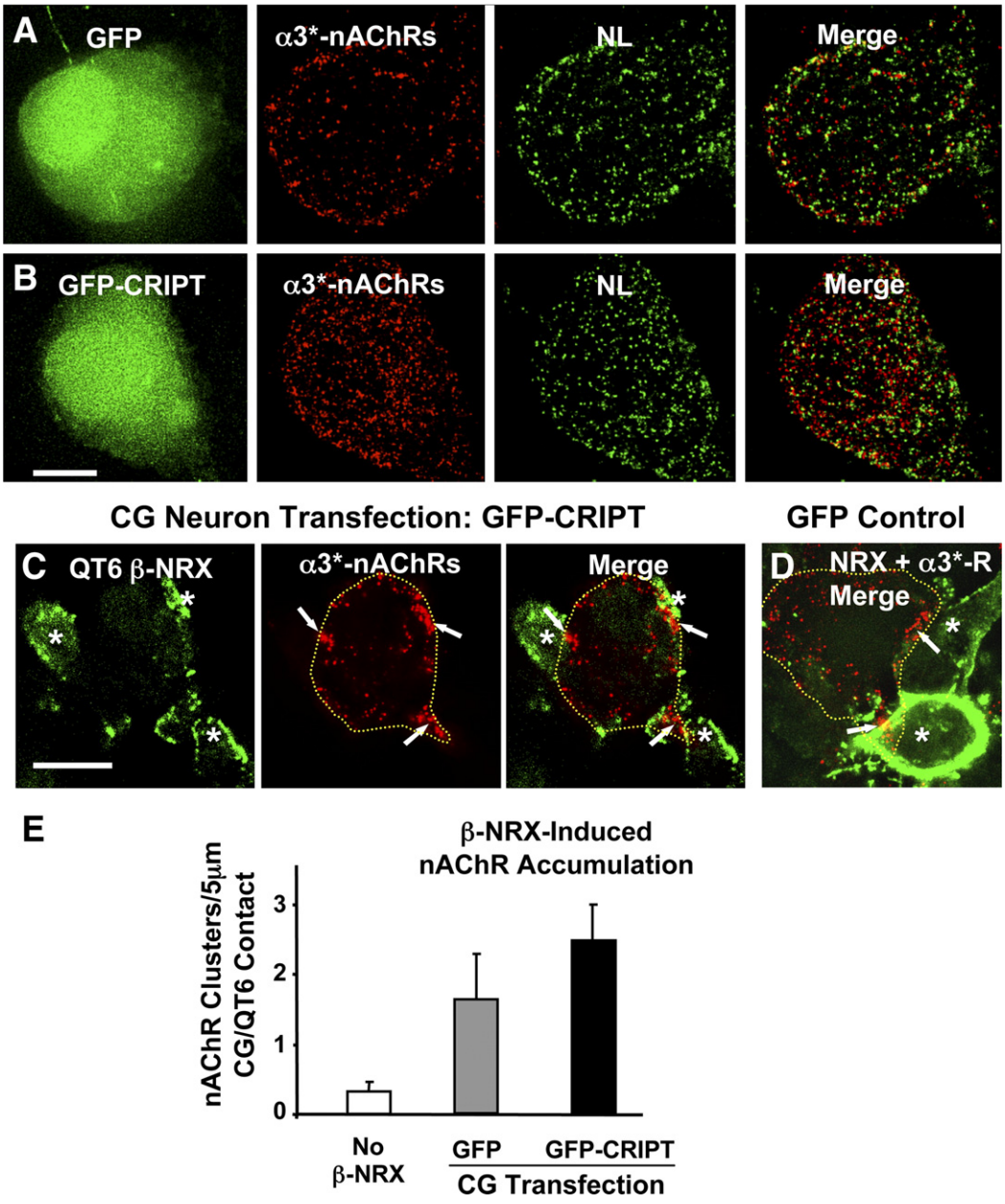

Fig. 7. NL actions in the absence of PDZ-scaffolds. E8 CG neurons were transfected with NL-1 and either GFP (A) or GFP-CRIPT (B). The neurons were stained for α3-nAChRs (red) and co-stained for transfected NL-1 (green in the third panels). Transfected NL-1 and α3*-nAChR showed comparable staining to GFP controls when PDZ-scaffolds were dispersed by CRIPT-GFP. Anti-PDZ staining confirmed that CRIPT dispersed the PDZ-complexes (not shown). CG neurons were also transfected with GFP-CRIPT to disrupt PDZ scaffolds (C) or with GFP as a negative control (D) and then co-cultured for 5–7 days with QT-6 cells transfected with β-NRX-1. Asterisks indicate β-NRX (green) transfected QT-6 cells; arrows indicate α3*-nAChR clusters (red) at CG neuron/QT-6 contact sites (Panel D) includes a particularly bright QT-6 cell). GFP fluorescence in the neurons is not shown. Neurons are outlined with hatched yellow lines. Merged images indicate the localization of receptor clusters at QT-6/neuron contacts for CRIPT- and GFP-transfected cells. (E) Quantification of α3*-nAChR clusters at QT-6/neuron contacts showed that GFP-CRIPT transfection of CG neurons did not diminish the ability of β-NRX-transfected cells to induce α3*-nAChR clusters, compared to negative controls using QT-6 cells transfected with GFP. Scale bars: 5 μm for panels A and B; 10 μm for panel C. The results suggest that β-NRX can act through endogenous NL to induce α3*-nAChR clusters even in the absence of PDZ-scaffolds.

transfection of NL with the CRIPT construct did not prevent the overlap (Fig. 7B). More importantly, cells transfected with β-NRX could still induce α3*-nAChR clusters on adjacent cells even when the adjacent cells were transfected with the CRIPT construct to disperse PDZ-scaffolds (Figs. 7C, D). Quantifying the incidence of α3*-nAChR clusters showed CRIPT-transfected cells to have at least as many receptor clusters at points of contact as do control GFP-transfected cells, and both values were significantly higher than those seen in control cells not contacted by β-NRX-transfected cells (Fig. 7E). The results show that even endogenous NL, when mobilized by sufficient β-NRX, can organize postsynaptic components in the absence of PDZ-scaffolds.

Role of endogenous NL

The finding that β-NRX-expressing cells and neurites can induce clustering of postsynaptic components in adjacent CG neurons strongly suggests that endogenous NL is available in the neurons and can enhance nicotinic input. Additional evidence attesting to the importance of endogenous NL and the significance of the cytoplasmic domain came from the results with the cytoplasmic fragment GFPCyNL54. As noted above (Fig. 6B), it acts as a dominant negative, reducing mEPSC frequency. A third line of evidence that endogenous NL contributes to nicotinic synapses in CG cultures was provided by knockdown experiments using RNA interference. An shRNA was designed to target the 417–437 nucleotides of chick NL-1 RNA. Co-transfecting HEK293 cells with NL-1 and the shRNA construct caused a significant decrement in the amount of NL-1 expressed compared with NL-1 expression alone, as detected by fluorescence immunohistochemistry (data not shown). A control RNA of similar length and composition but different sequence had no effect. Endogenous levels of NL-1 in CG neurons could not be assessed with the antibodies currently available. However, exposing CG neurons in culture to the shRNA for 7 days caused a 4-fold decrease in the frequency of mEPSCs measured in TTX (1.29±0.36 vs. 0.31±0.05 Hz for control vs. shRNA; $p \leq 0.05$; $n=18$ and 17 cells, respectively). No change was seen in the amplitude and time course of nicotine-induced whole-cell currents. The control RNA again had no effect on any of the parameters. These results are consistent with endogenous NL playing an important role in promoting nicotinic input to the neurons.

The mechanism by which endogenous NL affects mEPSC frequency, however, may differ from that employed by high levels of NL achieved by transfection. This view is suggested by the finding that shRNA expression did not reduce the number of SV2 clusters abutting the neuron even though the neuron displayed significantly fewer mEPSCs. SV2 clusters in this case were quantified using the same procedures employed for Fig. 3 (10.7±2.4 and 8.8±2.4 clusters for shRNA and untransfected, respectively; mean±SEM, $n=2$ cultures, 6 cells each; $p=0.55$ by Student's *t*-test). A similar conclusion was reached when SV2 clusters were quantified on neurons expressing the dominant negative construct ExFmsCyNL-pdz. Though the dominant negative significantly reduced the frequency of mEPSCs in transfected neurons, no difference was seen in the number of SV2 clusters abutting the soma of such cells (8.3± 3.4 and 9.0±1.1 clusters for ExFmsCyNL-pdz and GFP controls, respectively; mean±SEM with $n=5$ cultures containing 15 cells in both cases; $p=0.35$, Student's *t*-test). Endogenous NL is apparently not needed for the basal level of synapse formation that occurs in the cultures, as reflected by alignment of pre- and postsynaptic components. It is required, however, for optimal functionality of the contacts, perhaps exerting trans-synaptic effects on neurotransmitter release as recently suggested for NL at glutamatergic synapses (Futai et al., 2007). The high levels of NL found in transfected cells, on the other hand, do appear to induce additional synaptic contacts as judged both by immunostaining and by mEPSC frequency.

Discussion

The results reported here show that NL-1 can enhance nicotinic innervation of neurons. When expressed at high levels, it acts from the postsynaptic side to induce presynaptic specializations over postsynaptic nicotinic receptor clusters. The newly appearing synaptic contacts appear to be functional since they correlate with increased spontaneous mEPSCs in the neurons. The NL-1 acetylcholinesterase-like extracellular domain, which participates in trans interactions with β-NRX, is necessary to organize the presynaptic elements. The transmembrane/initial cytoplasmic domain of NL-1 is necessary to obtain active synaptic contacts. These early events in NL-induced synaptogenesis do not require interactions with postsynaptic PSD-95 family members, if the NL is present in sufficient abundance.

Staining for SV2 puncta provided strong evidence that NL-transfection increased the number of synapses formed on the neurons. More SV2 puncta were found on NL-transfected neurons and more were located over nAChR clusters, though NL produced no change in the number of nAChR clusters. In addition, NL-transfection increased the frequency of mEPSCs, suggesting that the increased synaptic contacts were functional. The results were not species-dependent: transfections with chick and rat NL-1 produced the same outcome. It is unlikely that NL-enhancement of mEPSC frequency simply resulted from rescue of events too small to detect in control cells. The mEPSCs were equivalent in amplitude for control and NL-transfected cells with the peak of events well above the size cutoff for event detection both for control and for NL-transfected populations.

Interestingly, endogenous NL also promotes nicotinic input to neurons but does not appear to determine the number of synaptic contacts, at least as judged by detectable alignment of pre- and postsynaptic elements. Both the shRNA experiments and those with dominant negatives indicated that endogenous NL was necessary to sustain the frequency of mEPSCs seen in control neurons. The fact that disruption of endogenous NL interactions did not also reduce the number of visually distinguished synaptic contacts suggests that other components in the neurons are sufficient for generating the basal level of contacts seen. Candidates include L1 and SynCAM, both of which are expressed in the neurons (Triana-Baltzer et al., 2006,

and unpublished results). Endogenous NL may be necessary to sustain mEPSC frequency at such synapses because it interacts with a presynaptic component to enhance the probability of transmitter release. NL effects on release probability have recently been documented for glutamatergic synapses (Futai et al., 2007). Notably, endogenous NL levels are sufficient to increase the number of synaptic contacts when organized by sufficient transcellular β-NRX. Thus cells expressing β-NRX not only induced visible clusters of endogenous NL in adjacent neurons at points of contact, but also increased the number of PSD-95/α3*-nAChR co-clusters at such sites.

The endogenous presynaptic molecular partner of NL in the present experiments with CG neurons in culture was very likely β-NRX. This is suggested both by the requirement for the NL-1 extracellular domain with the β-NRX binding site to obtain synaptogenesis, and by the RT–PCR demonstration of β-NRX transcript showing that the CG normally expresses it. Numerous studies in non-nicotinic pathways have shown that NL readily interacts with endogenous β-NRX on adjacent axons to assemble presynaptic transmitter release sites (Scheiffele et al., 2000; Dean et al., 2003; Graf et al., 2004; Chih et al., 2005; Chubykin et al., 2005; Levinson et al., 2005). In vivo, CG neurons are innervated by neurons from the accessory oculomotor nucleus (Dryer, 1994). A reasonable prediction, not yet testable, is that preganglionic neurons express β-NRX and traffic it to their axon terminals. The presence of β-NRX transcript in the CG indicates local synthesis as well. A possible role is that of direct postsynaptic regulation of NL as suggested recently for glutamatergic synapses (Taniguchi et al., 2007). Alternatively, the β-NRX may be destined for a presynaptic function at CG terminals in the periphery.

A major focus of the present work was the postsynaptic mechanism by which NL promotes synapse formation in nicotinic pathways. As noted above, the transmembrane/initial cytoplasmic domain of NL-1 was needed to enhance synaptic input. This is consistent with previous reports that the cytoplasmic domain is necessary for NL-1 synaptic targeting and co-localization with receptors in the cell membrane (Dresbach et al., 2004; Chih et al., 2005). The extracellular domain in those cases acted through β-NRX to induce presynaptic release sites while the initial cytoplasmic domain helped to align the presynaptic sites over postsynaptic receptors. NL-1 expressed in sufficient amounts or clustered by sufficient β-NRX can clearly increase nicotinic synapses without requiring an interaction with PSD-95 family members. One possibility is that NL/β-NRX interactions normally induce the initial events in synapse formation. This view would be consistent with several studies (Dean et al., 2003; Graf et al., 2004; Prange et al., 2004; Chih et al., 2005; Levinson et al., 2005), including an ultrastructural analysis of contacts formed by hippocampal neurons onto non-neuronal cells expressing NL-1. Not only were presynaptic components present in the axons but also postsynaptic membrane thickenings could be seen on the non-neuronal cells (Chubykin et al., 2005). Subsequent recruitment of PDZ-scaffolds could then increase the number of postsynaptic nAChRs as well as sequester signal transduction machinery, for synaptic maturation.

An alternative possibility is that NL/β-NRX interactions do not usually reach threshold for synapse formation unless augmented by supporting machinery. Postsynaptic PDZ-scaffolds may provide the additional clustering required to reach threshold for generating intercellular NL/β-NRX links. Support for this view comes from recent imaging studies on hippocampal neurons in culture showing that PDZ-complexes can contribute at early times to synapse formation (Gerrow et al., 2006). PDZ-scaffolds in this context would provide a regulatory role determining when and how many synapses were formed. Recent data from NL1–3 knockout mice (Varoqueaux et al., 2006) suggest that NLs are not required for initial synapse formation, but are necessary for the functional maturation of both excitatory and inhibitory synapses, presumably through the recruitment, assembly, and stabilization of pre- and postsynaptic proteins. PDZ-scaffold proteins could play an instructive role in combination with NLs, similar to that seen in neurons over-expressing PSD-95 where the ratio of excitatory-to-inhibitory synapses induced by NL-1 is increased (Graf et al., 2004; Prange et al., 2004; Chih et al., 2005; Levinson et al., 2005).

Support for the idea that NL plays a role in synaptic maturation, as opposed to initiation, also comes from the present studies which show that endogenous levels of NL enhance synaptic function without determining the number of visually distinguishable synaptic contacts. The postsynaptic PDZ-scaffold is important for maintaining the functional synapse in this case, as is shown by the fact that heterologous expression of CRIPT to disperse PDZ-clusters dramatically reduces nicotinic input to the neurons (Conroy et al., 2003). Endogenous NL levels are not sufficient to induce and sustain functional input to the neurons in the absence of assistance from the PDZ-scaffold and tethered components. Overexpressing NL or enhancing NL clustering by β-NRX overcomes this insufficiency, presumably because critical mass has been reached for NL interactions. We cannot exclude the possibility that even in this case the NL acts to stabilize synapses that are rapidly turning over. The results do indicate, however, that NL actions in the postsynaptic cell are important for nicotinic input and suggest at least two mechanisms by which this may occur, depending on the levels of NL and/or β-NRX available. The results also indicate that regulating the levels of NL and β-NRX expressed by neurons may be key in determining whether NL initiates synapse formation independent of PDZ-scaffolds and other controlling elements.

If NL can initiate synapse formation, the question arises as to how specificity is achieved in matching transmitter to receptor type. Though several NLs have been identified, it is clear that each is multipotent. Multiple naturally occurring NRX species can also contribute to synapse formation but their roles in synaptic specificity are not yet known (Boucard et al., 2005; Graf et al., 2006). If NL/β-NRX interactions initiate synaptic contacts in vivo, they may permit a promiscuity that allows the neuron to accommodate a variety of developmental outcomes initially. This flexibility would interface well with the reported ability of neurons to alter their transmitter commitment based on their level of excitability and calcium

signaling early in development (Borodinsky et al., 2004). Once functional matches occur between presynaptic transmitter and postsynaptic receptor, the resulting activity could direct subsequent events. The ability of PSD-95 levels to influence the balance between excitatory and inhibitory synapses induced by NL may be an example of this.

Acknowledgments

Grant support was provided by NIH Grants NS12601 and NS35469, and by Phillip Morris USA and Phillip Morris International. We thank Thomas Sudhof, Palmer Taylor, and Davide Comoletti for generously providing us the rat NL-1 and mouse NL-gpi constructs. We also thank Lynn Ogden and Xiao-Yun Wang for excellent technical assistance, Arin VanderVorst, David Ko, and Keith Gunapala for cell cultures, and Heather Eshleman, Taylor Berg-Kirkpatrick and Mimi Nguyen for biochemical and DNA work.

References

Boucard, A.A., Chubykin, A.A., Comoletti, D., Taylor, P., Sudhof, T.C., 2005. A splice code for trans-synaptic cell adhesion mediated by binding of neuroligin-1 to α- and β-neurexins. Neuron 48, 229–236.

Borodinsky, L.N., Root, C.M., Cronin, J.A., Sann, S.B., Gu, X., Spitzer, N.C., 2004. Activity-dependent homeostatic specification of transmitter expression in embryonic neurons. Nature 429, 523–530.

Chen, M., Pugh, P.C., Margiotta, J.F., 2001. Nicotinic synapses formed between chick ciliary ganglion neurons in culture resemble those present on the neurons in vivo. J. Neurobiol. 47, 265–279.

Chih, B., Engelman, H., Scheiffele, P., 2005. Control of excitatory and inhibitory synapses formation by neuroligins. Science 307, 1324–1328.

Chubykin, A.A., Liu, X., Comoletti, D., Tsigelny, I., Taylor, P., Sudhof, T.C., 2005. Dissection of synapse induction by neuroligins. Effect of a neuroligin mutation associated with autism. J. Biol. Chem. 280, 22365–22374.

Comoletti, D., Flynn, R., Jennings, L.L., Chubykin, A., Matsumura, T., Hasegawa, H., Sudhof, T.C., Taylor, P., 2003. Characterization of the interaction of a recombinant soluble neuroligin-1 with neurxin-1β. J. Biol. Chem. 278, 50497–50505.

Conroy, W.G., Berg, D.K., 1995. Neurons can maintain multiple classes of nicotinic acetylcholine receptors distinguished by different subunit compositions. J. Biol. Chem. 270, 4424–4431.

Conroy, W.G., Berg, D.K., 1998. Nicotinic receptor subtypes in the developing chick brain: appearance of a species containing the *α4*, *β2*, and *α5* gene products. Mol. Pharmacol. 53, 392–401.

Conroy, W.G., Liu, Z., Nai, Q., Coggan, J.S., Berg, D.K., 2003. PDZ-containing proteins provide a functional postsynaptic scaffold for nicotinic receptors in neurons. Neuron 38, 759–771.

Craig, A.M., Kang, Y., 2007. Neurexin–neuroligin signaling in synapse development. Curr. Opin. Neurobiol. 17, 43–52.

Dean, C., Scholl, F.G., Choih, J., DeMaria, S., Berger, J., Isacoff, E., Scheiffele, P., 2003. Neurexin mediates the assembly of presynaptic terminals. Nat. Neurosci. 6, 708–716.

Dresbach, T., Neeb, A., Meyer, G., Gundelfinger, E.D., Brose, N., 2004. Synaptic targeting of neuroligin is independent of neurexin and SAP90/PSD95 binding. Mol. Cell. Neurosci. 27, 227–235.

Dryer, S., 1994. Functional development of the parasympathetic neurons of the avian ciliary ganglion: a classic model system for the study of neuronal differentiation and development. Prog. Neurobiol. 43, 281–322.

Futai, K., Kim, M.J., Hashikawa, T., Scheiffele, P., Sheng, M., Hayashi, Y., 2007. Retrograde modulation of presynaptic release probability through signaling mediated by PSD-95–neuroligin. Nat. Neurosci. 10, 186–195.

Gerrow, K., Romorini, S., Nabi, S.M., Colicos, M.A., Sala, C., El-Husseini, A., 2006. A preformed complex of postsynaptic proteins is involved in excitatory synapse development. Neuron 49, 547–562.

Graf, E.R., Zhang, X.Z., Jin, S.-X., Linhoff, M.W., Craig, A.-M., 2004. Neurexins induce differentiation of GABA and glutamate postsynaptic specializations via neuroligins. Cell 119, 1013–1026.

Graf, E.R., Kang, Y., Hauner, A.M., Craig, A.M., 2006. Structure function and spice site analysis of the synaptogenic activity of the neurexin-1β LNS domain. J. Neurosci. 26, 4256–4265.

Ichtchenko, K., Hata, Y., Nguyen, T., Ullrich, B., Missler, M., Moomaw, C., Sudhof, T.C., 1995. Neuroligin 1: a splice site-specific ligand for β-neurexins. Cell 81, 435–443.

Ichtchenko, K., Nguyen, T., Sudhof, T.C., 1996. Structure, alternate splicing, and neurexin binding of multiple neuroligins. J. Biol. Chem. 271, 2676–2682.

Irie, M., Hata, Y., Takeuchi, M., Ichtchenko, K., Toyoda, A., Hirao, K., Takai, Y., Rosahl, T.W., Sudhof, T.C., 1997. Binding of neuroligins to PSD-95. Science 277, 1511–1515.

Levinson, J.N., Chery, N., Huang, K., Wong, T.P., Gerrow, K., Kang, R., Prange, O., Wang, Y.T., El-Husseini, A., 2005. Neuroligins mediate excitatory and inhibitory synapse formation. Involvement of PSD-95 and neurexin-1β in neuroligin-induced synaptic specificity. J. Biol. Chem. 280, 17312–17319.

Liu, Z., Tearle, A.W., Nai, Q., Berg, D.K., 2005. Rapid activity-driven SNARE-dependent trafficking of nicotinic receptors. J. Neurosci. 25, 1159–1168.

Nai, Q., McIntosh, J.M., Margiotta, J.F., 2003. Relating neuronal nicotinic acetylcholine receptor subtypes defined by subunit composition and channel function. Mol. Pharmacol. 63, 311–324.

Nam, C.I., Chen, L., 2005. Postsynaptic assembly induced by neurexin–neuroligin interaction and neurotransmitter. Proc. Natl. Acad. Sci. U. S. A. 102, 6137–6142.

Nishi, R., Berg, D.K., 1981. Two components from eye tissue that differentially stimulate the growth and development of ciliary ganglion neurons in cell culture. J. Neurosci. 1, 505–513.

Parker, M.J., Zhao, S., Bredt, D.S., Sanes, J.R., Feng, G., 2004. PSD93 regulates synaptic stability at neuronal cholinergic synapses. J. Neurosci. 24, 378–388.

Prange, O., Wong, T.P., Gerrow, K., Wang, Y.T., El-Husseini, A., 2004. A balance between excitatory and inhibitory synapses is controlled by PSD-95 and neuroligin. Proc. Natl. Acad. Sci. U. S. A. 101, 13915–13920.

Sanes, J.R., Lichtman, J.W., 2001. Induction, assembly, maturation and maintenance of a postsynaptic apparatus. Nat. Rev, Neurosci. 2, 791–805.

Scheiffele, P., Fan, J., Choih, J., Fetter, R., Serafini, T., 2000. Neuroligin expressed in nonneuronal cells triggers presynaptic development in contacting axons. Cell 101, 657–669.

Shoop, R.D., Martone, M.E., Yamada, N., Ellisman, M.H., Berg, D.K., 1999. Neuronal acetylcholine receptors with α7 subunits are concentrated on somatic spines for synaptic signaling in embryonic chick ciliary ganglia. J. Neurosci. 19, 692–704.

Shoop, R.D., Esquenazi, E., Yamada, N., Ellisman, M.H., Berg, D.K., 2002. Ultrastructure of a somatic spine mat for nicotinic signaling in neurons. J Neurosci. 22, 748–756.

Taniguchi, H., Gollan, L., Scholl, F.G., Mahadomrongkul, V., Dobler, E., Limthong, N., Peck, M., Aoki, C., Scheiffele, P., 2007. Silencing of neuroligin function by postsynaptic neurexins. J. Neurosci. 27, 2815–2824.

Triana-Baltzer, G.B., Liu, S., Berg, D.K., 2006. Pre- and postsynaptic actions of L1-CAM in nicotinic pathways. Mol. Cell. Neurosci. 33, 214–226.

Varoqueaux, F., Aramuni, G., Rawson, R.L., Mohrmann, R., Missier, M., Gottmann, K., Zhang, W., Sudhof, T.C., Brose, N., 2006. Neuroligins determine synapse maturation and function. Neuron 51, 741–754.

Williams, B.M., Tamburni, M.K., Schwartz, L.M, Bertrand, S., Bertrand, D., Jacob, M.H., 1998. The long internal loop of the α3 subunit targets nAChRs to subdomains within individual synapses on neurons in vivo. Nat. Neurosci. 1, 557–562.

Zhang, Z.-w., Vijayaraghavan, S., Berg, D.K., 1994. Neuronal acetylcholine receptors that bind α-bungarotoxin with high affinity function as ligand-gated ion channels. Neuron 12, 167–177.